End winding leakage calculation of a squirrel-cage induction motor for different load conditions

R. De Weerdt, K. Hameyer, R. Belmans
Dept. ESAT, Research Group ELEN
Kard. Mercierlaan 94, 3001 LEUVEN, BELGIUM

Abstract: The calculation of the end winding leakage of a squirrel-cage induction motor using a three-dimensional finite element method is discussed. The end winding inductance is thought to consist of a leakage, describing the flux linked with the end winding only, and a mutual part, describing the flux linked with both end winding and end ring. Both leakage and mutual inductance are found to vary for different load conditions.

Introduction

To analyse induction motors using the finite element method, a two-dimensional approach is most often used [1]. The motor end effects (end winding impedance and end ring impedance) are incorporated in the analysis as lumped parameters linked with the finite element model by a set of circuit equations. To incorporate the end winding and end ring inductance at the appropriate location in the coupled finite element - circuit model, these inductances have to be split into a leakage component and a mutual component. The mutual inductance is part of the magnetising inductance but can be neglected in practise since the coupling is in air. Determining both leakage components using an analytical or empirical approach is not possible. Furthermore, the analytical approximations assume the end winding leakage to be constant for all operating conditions [2]. It is shown that this assumption is incorrect. The leakage inductance is found to decrease when the load increases due to the increase of the mutual inductance between end winding and end ring.

3D finite element model

The finite element analysis is performed using a commercial CAD package [3]. The 3D mesh is generated by extrusion. An axial cross-section of the end winding region of the motor is used as the base plane (figure 1). This base-plane has to contain all outlines required in the final model. The consecutive planes are generated by rotating the base plane around the center line of the shaft. 84 planes are required to generate the 3D model.

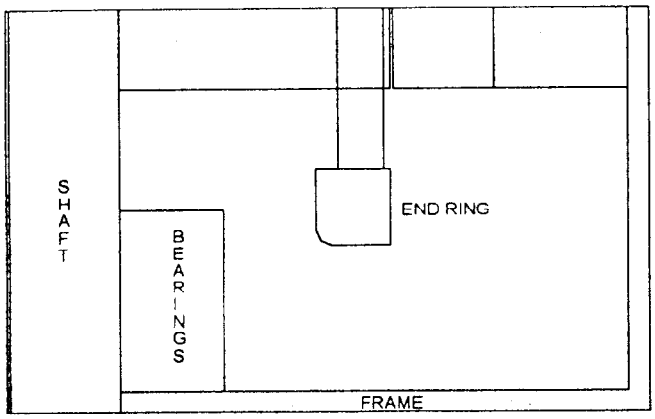

Fig. 1: Axial cross-section of the end winding region

By relabeling the different regions in the consecutive planes, the 3D model is built. An other set of meshes represents the current excited coils and is joined with the material mesh, i.e. the 3D model generated from the base plane, during the problem definition. Due to symmetry, only one quarter of one end region has to be modelled. Figure 2 shows part of the material mesh (the end ring and rotor bar ends) together with the stator end winding coils.

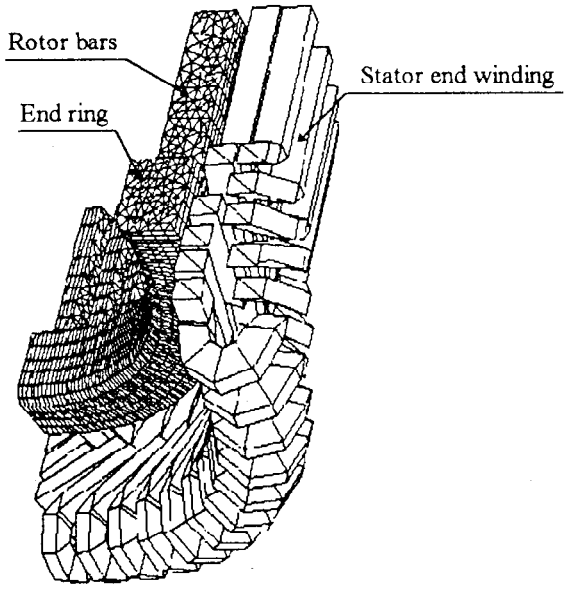

Fig. 2: 3D model of one quarter of an end winding region of a squirrel cage induction motor

Referring to figure 2, it is obvious that the generation of the stator end winding coils requires a more complex extrusion based model compared to the material mesh. Therefore, the building of such complex models using extrusion techniques is only possible if material and coil meshes can be treated separately. The rotor coil meshes, required for the definition of the rotor excitation, are located inside the end ring and rotor bar ends.

Inductance calculations

The inductances are calculated based on the stored energy in the model [4]. To determine both leakage components and the mutual inductance three problems have to be solved. One having only the stator coils excited, one having only the rotor coils excited and one problem with both stator and rotor coils excited. Considering the stored energy in these problems to be W_{m1}, W_{m2} and W_{m3}, the following equations are valid:

$$W_{m1} = \frac{m}{2}\frac{1}{8}L_s i_1^2$$

$$W_{m2} = \frac{1}{2*4}L_r i_r^2 = \frac{m}{2}\frac{1}{8}L_r'(i_r')^2 \qquad (1)$$

$$W_{m3} = \frac{m}{2}\frac{1}{8}L_s i_1^2 + \frac{m}{2}\frac{1}{8}L_r'(i_r')^2 \pm \left(\frac{m}{2}\frac{1}{8}M_{rs} i_1 i_r' + \frac{m}{2}\frac{1}{8}M_{sr} i_1 i_r'\right)$$

L_s: stator end winding inductance, L_r: end ring inductance, L_r' : end ring inductance referred to the stator, i_r: ring current, i_r' : ring current referred to the stator, i_1: stator current, M_{rs} and M_{sr}: mutual inductance between stator end winding and rotor end ring, and m the number of phases (m = 3).
Since the rotor values are referred to the stator, $M_{rs} = M_{sr} = M$. The value of W_{m3} is less than $(W_{m1} + W_{m2})$ (the negative sign has to be applied in the expression for W_{m3}) if the flux caused by the rotor excitation opposes the stator flux. If the rotor flux supports the stator flux, W_{m3} will be higher than $(W_{m1} + W_{m2})$. Under normal conditions, the rotor flux opposes the stator flux, resulting in $W_{m3} < (W_{m1} + W_{m2})$. The division by eight or four in equation (1) takes into account that only one fourth of one end region or one fourth of one end ring is modelled.

When only the mutual inductance has to be calculated, it is sufficient to solve two problems, one with the rotor flux opposing the stator flux, one with the rotor flux supporting the stator flux. The difference between both stored energy values is only a function of the mutual inductance and the applied currents [4]. Introducing the stator end winding leakage, $L_{\sigma s}$, the end ring leakage, $L_{\sigma r}$ and the end ring leakage referred to the stator, $L_{\sigma r}'$, the different inductances can be calculated from

$$L_s = W_{m1}\frac{2}{m}\frac{8}{i_1^2} \qquad L_{\sigma s} = L_s - M$$

$$L_r' = W_{m2}\frac{2}{m}\frac{8}{(i_r')^2} \qquad L_{\sigma r}' = L_r' - M$$

$$L_r = W_{m2}\frac{2*4}{i_r^2} \qquad L_{\sigma r} = L_r\frac{L_{\sigma r}'}{L_r'} = L_r\left(1 - \frac{M}{L_r'}\right) \qquad (2)$$

$$M = (W_{m3} - W_{m1} - W_{m2})\frac{8}{3 i_1 i_r'}$$

Results

The following table shows the calculated inductances at three different slip values. A linear time-harmonic solution is used. Therefore, the self inductance of end winding L_s and end ring L_r remain constant.

Table 1: Calculated inductance components at different slip values

Inductance	slip [%]		
[mH]	0.34	1.42	100
L_s	0.49	0.49	0.49
L_r'	0.46	0.46	0.46
L_r	0.65e-3	0.65e-3	0.65e-3
M	0.13	0.19	0.21
$L_{\sigma r}'$	0.33	0.30	0.25
$L_{\sigma r}$	0.47e-3	0.42e-3	0.35e-3
$L_{\sigma s}$	0.36	0.30	0.28

From table 1, a decrease of the leakage and an increase of the mutual inductance is noticed. At no load, the full self inductance of the motor is considered as leakage resulting in a leakage inductance of this motor with a variation from 0.49 mH at no load to 0.28 mH at locked rotor.

Conclusions

The end winding inductance of a squirrel cage induction motor is calculated using a 3D finite element method. A significant variation of the leakage components of both end winding and end ring inductance is found at different load situations.

Acknowledgement

The authors express their gratitude to the Belgian Ministry of Scientific Research for granting the IUAP No. 51 on Magnetic Fields, to Holec, Machines & Apparaten, Ridderkerk and to the Council of the Belgian National Science Foundation.

References

[1] E. Vassent, G. Meunier, J.C. Sabonnadiere: "Simulation of induction machine operation using complex magnetodynamic finite elements", *IEEE Trans. on Magnetics*, Vol. 25, No. 4, 1989, pp. 3064-3066.

[2] W. Nürnberg: *Die Asynchronmaschine*, Springer Verlag Berlin Heidelberg New York, 1952.

[3] E.M. Freeman: *MagNet User Guide*, Infolytica Montreal, 1994

[4] A.Lowther, P.P.Silvester: *Computer-Aided Design in Magnetics*, Springer-Verlag, New York, 1985.